Low-voltage-tunable nanobeam lasers immersed in liquid crystals

Sejeong Kim,[1] Hwi-Min Kim,[1] Jaehyun Son,[2] Yun-Ho Kim,[3] Jong Min Ok,[4] Ki Soo Kim,[5] Hee-Tae Jung,[4] Bumki Min,[2] and Yong-Hee Lee[1,6,*]

[1]*Department of Physics, Korea Advanced Institute of Science and Technology, Daejeon 305-701, South Korea*
[2]*Department of Mechanical Engineering, Korea Advanced Institute of Science and Technology, Daejeon 305-701, South Korea*
[3]*Advanced Functional Materials Research Group, Korea Research Institute of Chemical Technology, Daejeon 305-600, South Korea*
[4]*Department of Chemical and Biomolecular Engineering (BK21 + Program), Korea Advanced Institute of Science and Technology, Daejeon 305-701, South Korea*
[5]*Convergence and Component& Materials Research Laboratory, Electronics and Telecommunications Research Institute, Daejeon 305-700, South Korea*
[6]*Graduate School of Nanoscience and Technology (WCU), Korea Advanced Institute of Science and Technology, Daejeon 305-701, South Korea*
[*]*yhlee@kaist.ac.kr*

Abstract: A low-voltage-tunable one-dimensional nanobeam laser is realized by employing lithographically defined lateral electrodes. An InGaAsP nanobeam with a sub-micrometer width is transfer-printed in the middle of two electrodes using a polydimethylsiloxane stamp. Spectral tuning is achieved by controlling the molecular alignment of the surrounding liquid crystals (LCs). From μm-scale-gap structures, a total wavelength shift that exceed 6 nm is observed at a low voltage of less than 10 V. A measured spectral tuning rate of 0.87 nm/V, which is the largest value ever reported to our knowledge among LC-tuned photonic crystal lasers, was also noted.

©2014 Optical Society of America

OCIS codes: (160.5298) Photonic crystals; (140.5960) Semiconductor lasers; (160.3710) Liquid crystals; (140.3600) Lasers, tunable.

References and links

1. O. Painter, R. K. Lee, A. Scherer, A. Yariv, J. D. O'Brien, P. D. Dapkus, and I. Kim, "Two-dimensional photonic band-gap defect mode laser," Science **284**(5421), 1819–1821 (1999).
2. S. Noda, "Applied physics. Seeking the ultimate nanolaser," Science **314**(5797), 260–261 (2006).
3. K.-Y. Jeong, Y.-S. No, Y. Hwang, K. S. Kim, M.-K. Seo, H.-G. Park, and Y.-H. Lee, "Electrically driven nanobeam laser," Nat. Commun. **4**, 2822 (2013).
4. T.-W. Lu, L.-H. Chiu, P.-T. Lin, and P.-T. Lee, "One-dimensional photonic crystal nanobeam lasers on a flexible substrate," Appl. Phys. Lett. **99**(7), 071101 (2011).
5. B. Ellis, M. A. Mayer, G. Shambat, T. Sarmiento, J. Harris, E. E. Haller, and J. Vučković, "Ultralow-threshold electrically pumped quantum-dot photonic-crystal nanocavity laser," Nat. Photonics **5**(5), 297–300 (2011).
6. S. Kita, S. Hachuda, S. Otsuka, T. Endo, Y. Imai, Y. Nishijima, H. Misawa, and T. Baba, "Super-sensitivity in label-free protein sensing using a nanoslot nanolaser," Opt. Express **19**(18), 17683–17690 (2011).
7. B. Maune, J. Witzens, T. Baehr-Jones, M. Kolodrubetz, H. Atwater, A. Scherer, R. Hagen, and Y. Qiu, "Optically triggered Q-switched photonic crystal laser," Opt. Express **13**(12), 4699–4707 (2005).
8. W. S. Fegadolli, J. E. B. Oliveira, V. R. Almeida, and A. Scherer, "Compact and low power consumption tunable photonic crystal nanobeam cavity," Opt. Express **21**(3), 3861–3871 (2013).
9. S. W. Leonard, H. M. van Driel, J. Schilling, and R. B. Wehrspohn, "Ultrafast band-edge tuning of a two-dimensional silicon photonic crystal via free-carrier injection," Phys. Rev. B **66**(16), 161102 (2002).
10. M. W. Lee, C. Grillet, C. L. C. Smith, D. J. Moss, B. J. Eggleton, D. Freeman, B. Luther-Davies, S. Madden, A. Rode, Y. Ruan, and Y.-H. Lee, "Photosensitive post tuning of chalcogenide photonic crystal waveguides," Opt. Express **15**(3), 1277–1285 (2007).
11. A. Faraon, D. Englund, D. Bulla, B. Luther-Davies, B. J. Eggleton, N. Stoltz, P. Petroff, and J. Vuckovic, "Local tuning of photonic crystal cavities using chalcogenide glasses," Appl. Phys. Lett. **92**(4), 043123 (2008).
12. D. Sridharan, R. Bose, H. Kim, G. S. Solomon, and E. Waks, "A reversibly tunable photonic crystal nanocavity laser using photochromic thin film," Opt. Express **19**(6), 5551–5558 (2011).

#223484 - $15.00 USD Received 19 Sep 2014; revised 11 Nov 2014; accepted 17 Nov 2014; published 3 Dec 2014
(C) 2014 OSA

13. D. Erickson, T. Rockwood, T. Emery, A. Scherer, and D. Psaltis, "Nanofluidic tuning of photonic crystal circuits," Opt. Lett. **31**(1), 59–61 (2006).
14. I. C. Khoo, Y. Williams, A. Diaz, K. Chen, J. A. Bossard, L. Li, D. H. Werner, E. Graugnard, J. S. King, S. Jain, and C. J. Summers, "Liquid-crystals for tunable photonic crystals, frequency selective surfaces and negative index material development," Mol. Cryst. Liq. Cryst. (Phila. Pa.) **453**(1), 309–319 (2006).
15. B. Maune, M. Lončar, J. Witzens, M. Hochberg, T. Baehr-Jones, D. Psaltis, A. Scherer, and Y. Qiu, "Liquid-crystal electric tuning of a photonic crystal laser," Appl. Phys. Lett. **85**(3), 360–362 (2004).
16. S. W. Leonard, J. P. Mondia, H. M. van Driel, O. Toader, S. John, K. Busch, A. Birner, U. Gosele, and V. Lehman, "Tunable two-dimensional photonic crystals using liquid-crystal infiltration," Phys. Rev. B **61**(4), R2389–R2392 (2000).
17. Ch. Schuller, F. Klopf, J. P. Reithmaier, M. Kamp, and A. Forchel, "Tunable photonic crystals fabricated in III-V semiconductor slab waveguides using infiltrated liquid crystals," Appl. Phys. Lett. **82**(17), 2767–2769 (2003).
18. A. Casas Bedoya, S. Mahmoodian, C. Monat, S. Tomljenovic-Hanic, C. Grillet, P. Domachuk, E. C. Mägi, B. J. Eggleton, and R. W. van der Heijden, "Liquid crystal dynamics in a photonic crystal cavity created by selective microfluidic infiltration," Opt. Express **18**(26), 27280–27290 (2010).
19. M. A. Dündar, H. H. J. E. Kicken, A. Yu. Silov, R. Nötzel, F. Karouta, H. W. M. Salemink, and R. W. van der Heijden, "Birefringence-induced mode-dependent tuning of liquid crystal infiltrated InGaAsP photonic crystal nanocavities," Appl. Phys. Lett. **95**(18), 181111 (2009).
20. M. Ozaki, Y. Shimoda, M. Kasano, and K. Yoshino, "Electric field tuning of the stop band in a liquid-crystal-infiltrated polymer inverse opal," Adv. Mater. **14**(7), 514–518 (2002).
21. D. Ko, S. M. Morris, A. Lorenz, F. Castles, H. Butt, D. J. Gardiner, M. M. Qasim, B. Wallikewitz, P. J. W. Hands, T. D. Wilkinson, G. A. J. Amaratunga, H. J. Coles, and R. H. Friend, "A nano-patterned photonic crystal laser with a dye-doped liquid crystal," Appl. Phys. Lett. **103**(5), 051101 (2013).
22. A. S. P. Chang, H. T. H. Tan, S. Bai, W. W. W. Wu, Z. Y. Z. Yu, and S. Y. Chou, "Tunable external cavity laser with a liquid-crystal subwavelength resonant grating filter as wavelength-selective mirror," IEEE Photon. Technol. Lett. **19**(14), 1099–1101 (2007).
23. C.-Y. Liu and L.-W. Chen, "Tunable band gap in a photonic crystal modulated by a nematic liquid crystal," Phys. Rev. B **72**, 145133 (2005).
24. L. Criante and F. Scotognella, "Low-voltage tuning in a nanoparticle/liquid crystal photonic structure," J. Phys. Chem. C **116**(40), 21572–21576 (2012).
25. S. Kim, B.-H. Ahn, J.-Y. Kim, K.-Y. Jeong, K. S. Kim, and Y.-H. Lee, "Nanobeam photonic bandedge lasers," Opt. Express **19**(24), 24055–24060 (2011).
26. C.-S. Yang, C.-J. Lin, R.-P. Pan, C. T. Que, K. Yamamoto, M. Tani, and C.-L. Pan, "The complex refractive indices of the liquid crystal mixture E7 in the terahertz frequency range," J. Opt. Soc. Am. B **27**(9), 1866 (2010).

1. Introduction

In recent years, microlasers and microresonators with integrated optical systems have been studied and developed steadily [1–5]. Among the diverse characteristics of lasers, spectral tunability is a sought-after feature, as the resonant wavelength is often mismatched with the desired wavelength due to unavoidable fabrication imperfections. Also, a tunable laser itself is one of the most critical components of integrated photonic chips [6,7].

Various methods to tune the resonant wavelengths of laser cavities have been investigated. Several groups have taken advantage of thermo-optic effects or free-carrier effects [8,9]. Other groups employed materials such as chalcogenide glass [10,11], photochromic thin film [12], and micro-fluid [13]. Among the wide range of post-trimming methods of spectral tuning, those based on liquid crystals (LCs) offer several advantages [14]. First, they are sensitive to external electric fields on account of the very large electro-optic coefficients of LCs. Second, the considerable anisotropy of the LCs enables a wider tuning range in comparison to other methods. Third, LCs are optically transparent and compatible with semiconductors, and liquid-phase LCs allow for easy infiltration into the small air voids of photonic nanostructures. Numerous studies which demonstrate LC-infiltrated photonic crystal structures have been conducted thus far [15–23]. In previous experiments, however, relatively high tuning voltages had to be applied to introduce sufficient electric fields due to the large electrode gap. The capability of spectral tuning at a lower voltage is directly related to the total power consumption of an optical system and is a feature that goes well with photonic integrated circuits [24].

We propose a nematic LC-infiltrated nanobeam laser with lateral electrodes suitable for low-voltage operation. A lithographically defined planar style of the electrode geometry is chosen instead of the conventional vertical electrode geometry, and a more compact cavity

#223484 - $15.00 USD Received 19 Sep 2014; revised 11 Nov 2014; accepted 17 Nov 2014; published 3 Dec 2014
(C) 2014 OSA

structure is realized. In this study, a maximum tuning rate of 0.87 nm/1.0V is obtained with a threshold voltage of less than 1.0V.

2. Device design and simulation

To generate electric fields across electrodes and through a laser, a stick-like nanobeam resonator is inserted between two micron-gap-patterned gold electrodes, as shown in Fig. 1(a). The nanobeam is made of InGaAsP material with a lattice constant (*a*) of 350 nm, a width (*w*) of 525 nm and a thickness (*t*) of 280 nm. Fifty perforated airholes are used in the photonic crystal laser. The dielectric band edge mode with the lowest frequency is used, as shown in Fig. 1(b) owing to the good spatial overlap between the dielectric mode and the active gain medium [25]. Our horizontal planar geometry enables control of the electrode gap size to a range of less than 100 nm.

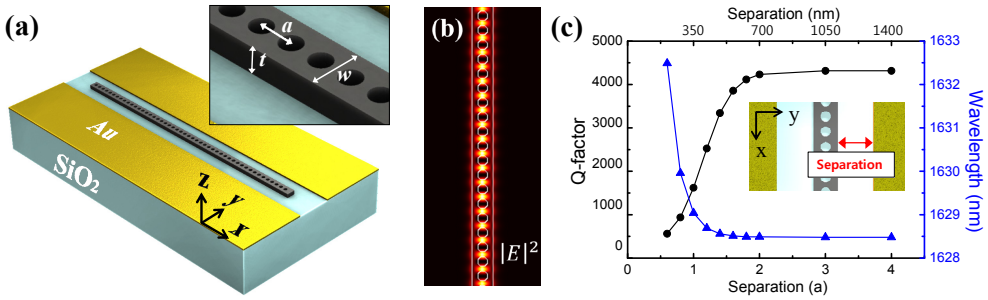

Fig. **1.** (a) Scheme of the device to realize a tunable nanobeam laser with electrodes. (b) Electric field intensity of the 0th dielectric bandedge mode. (c) Q-factor and resonant wavelength plot as a function of the degree of separation.

The calculated resonant wavelengths and Q-factors are plotted as functions of the degree of separation in Fig. 1(c). Here, the separation is defined as the distance between the edge of the nanobeam and the gold electrode, as shown in the inset of Fig. 1(c). The finite-difference time-domain (FDTD) simulation conducted here includes a nanobeam (n = 3.4) and gold electrodes on a glass substrate (n = 1.44) immersed in liquid crystals (n = 1.7). When the separation distance exceeds 700 nm, the Q-factor and the resonant wavelength remain unchanged. However, as the metal approaches the nanobeam, the evanescent field of the optical mode touches the absorptive metal and the resonant mode becomes lossy. At the same time, the effective refractive index increases and the lasing wavelength becomes red-shifted. Simulation results show that a separation distance of 350 nm continues to support a Q-factor of 1,400, meaning that the overall electrode gap size can be as small as 1 μm.

In our structure, the liquid crystals cover the nanobeam from the top and fill in the air voids of the nanobeam. The dependence of the quality factor and the wavelength on the surrounding refractive index is simulated in Fig. 2(a). Two principal refractive indices, the ordinary index (n_o = 1.502) and the extraordinary index (n_e = 1.688) of the nematic LC E7 (Merck) material are indicated in the figure with dashed lines [26]. E7 is selected in this study

#223484 - $15.00 USD Received 19 Sep 2014; revised 11 Nov 2014; accepted 17 Nov 2014; published 3 Dec 2014
(C) 2014 OSA

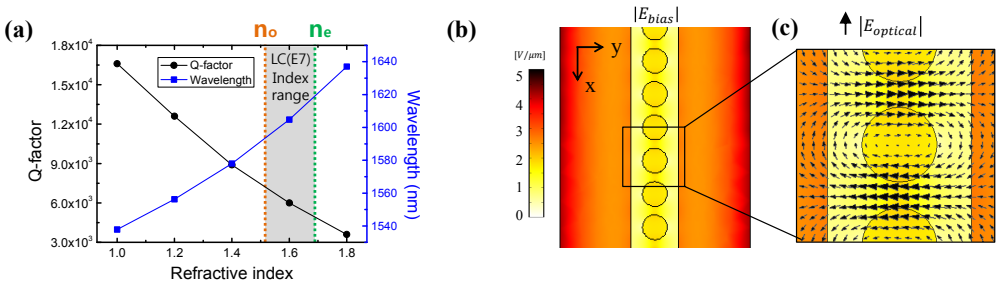

Fig. **2.** (a) Simulation result of the Q-factor and the resonant wavelength as a function of the surrounding refractive index. The refractive index of E7 (Merck) is represented. (b) Top view of the device with a normalized electric field magnitude when external voltage is applied. (c) The arrows indicate the electric field of the optical mode in the middle of the slab.

due to its relatively large index difference at 1.55 μm, which corresponds to 0.186 (0.217 in the visible wavelength) and due to its low clearing temperature of 58°C. Figure 2(a) reveals that the nanobeam when submerged in E7 holds a Q-factor larger than 4,000. Additionally, the magnitude of the electric field between two gold electrodes is plotted in Fig. 2(b). This 3D computation is performed with 100 nm-thick gold electrodes with a 2-μm-gap on a glass substrate. The colors in the plot represent the normalized electric field magnitude on the x-y plane with z at the center of the nanobeam slab. The electric fields are strong near the air-gold interface and weak in the air holes. The electric field of the dielectric bandedge mode is shown in Fig. 2(c) with black arrows. In this mode, E_y-field is dominant and the optical mode experiences mainly an ordinary refractive index associated with those LC molecules aligned along the z direction. In the same manner, the optical mode mainly overlaps with an extraordinary refractive index of the LC molecules aligned along the y direction. The theoretical maximum wavelength shift is estimated to be ~12 nm from FDTD simulations using the anisotropy refractive index in the surrounding material. Here, we assume that the resonant wavelength of the nanobeam cavity is 1,550 nm and that the LC orientation in the zero-electric field is completely vertical (z direction).

3. Fabrication and experimental results

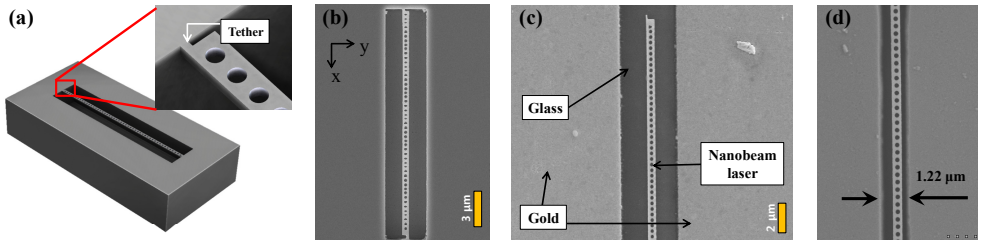

Fig. **3.** (a) Schematic of an InGaAsP nanobeam with tethers. (b) SEM image of a fabricated nanobeam with tethers. (c) SEM image of a transfer-printed nanobeam between gold electrodes. (d) A demonstration of a nanobeam in the narrow gold electrode gap.

An InGaAsP nanobeam with three layers of quantum wells in the middle of a slab is patterned by means of electron beam lithography [25]. The InP sacrificial layer is removed using diluted HCl solution to create freestanding structures, as shown in Fig. 3(a). Tethers are intentionally patterned at the end of the nanobeam to allow the nanobeam to be easily released from its parent chip. Figure 3(b) shows an SEM image of the nanobeam. Electrodes are prepared by depositing Cr (5 nm) and Au (100 nm) onto a glass substrate. The distance between the two electrodes is determined by e-beam lithography and Ar milling. The nanobeam structure is then transferred between the gold electrodes, as shown in Fig. 3(c), by using a transfer-printing technique. With our planar electrode geometry, the gap size of the electrodes can be

#223484 - $15.00 USD Received 19 Sep 2014; revised 11 Nov 2014; accepted 17 Nov 2014; published 3 Dec 2014
(C) 2014 OSA

pushed to the limit, where the evanescent field of the guided mode begins to sense the lossy metallic electrodes. One of the nanobeams successfully transfer-printed in the narrow gap is shown in Fig. 3(d).

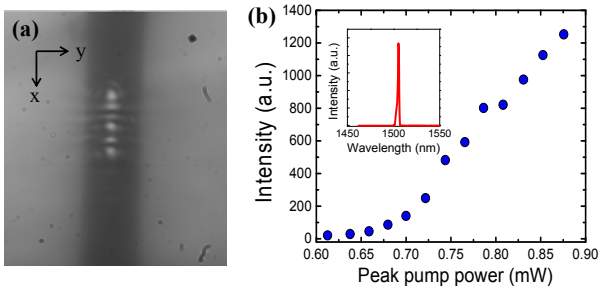

Fig. **4.** (a) Infrared CCD camera image of a lasing pattern from nanobeam with E7. (b) Light-in versus light-out curve of the nanobeam laser with E7 at a zero-electric field. (The inset shows the photoluminescence of the nanobeam.)

Nematic liquid crystals (E7 (Merck)) are employed in our experiment. To ensure that the LCs are fully infiltrated into the air voids of the nanobeam, the nanobeam and the E7 material are heated up to the nematic-isotropic transition temperature (58°C). Figures 4(a) and 4(b) show the characteristics of the laser. The measured peak pump power at the threshold was found to be ~0.7 mW at a wavelength of 1,505 nm (inset).

In order to study the spectral tunability, external voltage is applied to control the orientation of the molecular LC directors. Data measured with an electrode gap of 3.08 μm and 1.54 μm are shown in Fig. 5(a). When a 1-kHz rectangular AC electric field is applied, the resonance wavelength shows a red shift. This is attributed to the increased effective refractive index in response to the applied electric field. The total wavelength shift is greater with the nanobeam placed between the 1.54-μm gap compared to when it is positioned in the 3.08-μm gap. With the 1.54-μm-gap sample, a total wavelength shift of 6.2 nm is measured at 10.0 V. The threshold voltage of the LC is observed at ~1 V. The corresponding spectral tuning rate is 0.87 nm/1.0V in the linear regime (1~5 V). This spectral tuning rate can be improved even further if the gap size is reduced. Note that the threshold voltage is lower in a narrower gap because this condition generates the minimum electric field required for LCs to rotate at a lower voltage. The tuning processes for the samples with 1.54 μm and 3.08 μm gaps were found to be reversible with no hysteresis, as shown in the Figs. 5(b) and 5(c), respectively. Additionally, we noted that the resonant wavelength and line width are scarcely affected by the driving frequency, as shown in Fig. 5(d). Each data point in Fig. 5(d) is integrated for 0.25 second. The spectral tuning rate is plotted in Fig. 5(e) as a function of the applied electric field. The wavelength shift versus the electric field shows no electrode gap dependency, as the LCs respond to the electric field rather than the applied voltage. Subsequently, an experiment with DC voltage was also carried out, as presented in Fig. 5(f). In this case, the spectral tuning rate is 1.3 nm/V, which is even higher than the spectral tuning rate of the AC voltage. However, the use of the AC scheme is recommended to avoid ionic build-ups in LCs. Note that the total wavelength shift is not saturated, even at an AC voltage of 10 V and a DC voltage of 5 V, indicating that a further wavelength shift is possible.

#223484 - $15.00 USD Received 19 Sep 2014; revised 11 Nov 2014; accepted 17 Nov 2014; published 3 Dec 2014
(C) 2014 OSA

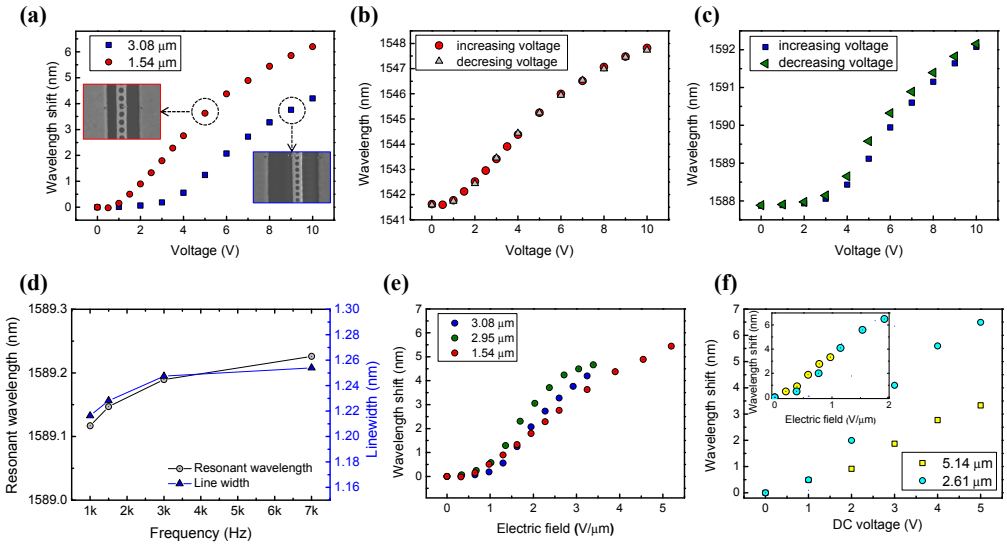

Fig. **5.** (a) Red-shift of the lasing wavelength versus the applied AC voltage. Reversible tuning is demonstrated in the samples with gap distances of (b) 1.54 μm and (c) 3.08 μm. (d) Resonant wavelength and line width versus the applied frequency of 50~7000 Hz. (e) Wavelength shift vs applied electric field. (f) Red shift of the lasing wavelength versus the applied DC voltage. The inset shows the wavelength shift versus the DC electric field.

4. Conclusion

In summary, we propose and demonstrate a low-voltage tunable nanobeam laser immersed in LCs by employing a planar electrode type of geometry. A spectral tuning rate of 0.87 nm/V is achieved, the highest ever recorded to the best of our knowledge. A total wavelength shift of more than 6 nm and a threshold LC voltage of 1V are obtained experimentally. Planar electrodes with a narrower gap enable the LCs to sense the same level of an electric field at a reduced voltage. Our scheme is advantageous for fabrication that electrodes with narrow-gaps can be easily and precisely defined using the state-of-the-art nanolithography.

Acknowledgment

This work was supported by the National Research Foundation of Korea (NRF) Grants funded by the Korea government (MEST) (2013K1A1A2035662, 2007-0093863)

#223484 - $15.00 USD Received 19 Sep 2014; revised 11 Nov 2014; accepted 17 Nov 2014; published 3 Dec 2014
(C) 2014 OSA